Available online at www.sciencedirect.com
SCIENCE DIRECT®
Journal of Sound and Vibration 274 (2004) 297–321
JOURNAL OF SOUND AND VIBRATION
www.elsevier.com/locate/jsvi

Transmission of vibration to the backrest of a car seat evaluated with multi-input models

Y. Qiu, M.J. Griffin*

Human Factors Research Unit, Institute of Sound and Vibration Research, University of Southampton, Highfield, Southampton SO17 1BJ, UK

Received 27 June 2002; accepted 20 May 2003

Abstract

The transmission of vibration to the occupant of a car seat has been studied using the multiple vibration inputs to the seat. Twelve input signals at the seat base (tri-axial vibration at the four corners) and six output signals (tri-axial vibration at the backrest and seat pan) were measured while driving. The results showed that vibration inputs to the seat varied between the four positions at the seat base. The two fore-aft input accelerations at the left-hand side of the seat base and the two fore-aft input accelerations at the right-hand side of the seat base were highly correlated with each other. There was also a high correlation between the two pairs of lateral acceleration inputs at the front and rear of the seat base. A computer program for studying seat vibration transmission via multi-input channels was developed to allow the calculation of seat transmissibility with up to 12 different inputs. The transmission of multi-axis seat base vibration to fore-aft seat backrest vibration was investigated using single-input, two-input, six-input and eight-input models. Results showed that the fore-aft vibration and the vertical vibration, but not lateral vibration, at the four corners of the seat base contributed to fore-aft vibration of the backrest. The primary peak of the fore-aft backrest transmissibility occurred around 4–5 Hz. The coherency was improved when using the multi-input models, although the characteristics of the transmissibility remained similar. The transmission of lateral vibration at the seat base to lateral vibration at the backrest was studied using single-input and two-input models. With single-input models, the transmission of lateral acceleration at the seat base to lateral acceleration at the backrest was amplified between 18 and 35 Hz, with a peak at 26 Hz. Coherency was greater at frequencies above 20 Hz than at lower frequencies. The coherency at low frequencies was increased with a two-input model. The transmission of vertical vibration to vertical vibration at the backrest was investigated using single-input, four-input and six-input models. The results showed that vertical acceleration at the four corners of the seat base was highly correlated with vertical acceleration at the backrest. The results are consistent with previous findings that a single-input model is not sufficient to study the transmission of vibration to the seat back in the horizontal directions, while for the transmission

*Corresponding author. Tel.: +44-23-8059-2277; fax: +44-23-8059-2927.
E-mail address: m.j.griffin@soton.ac.uk (M.J. Griffin).

0022-460X/$ - see front matter
doi:10.1016/j.jsv.2003.05.015

of vertical vibration a single-input model is probably sufficient, especially when low frequencies are of main concern.

1. Introduction

The vibration experienced when riding in a vehicle may be greatly affected by the manner in which the vibration is attenuated or amplified by the seat [1,2]. It has often been assumed that the vertical vibration transmitted through the seat cushion is the main contribution to vibration discomfort. Various studies have shown that in many cars seat cushions amplify vertical vibration below about 6 Hz, and have a resonance around 4 Hz [1]. The minimization of vibration discomfort in a car involves the optimization of the seat dynamics so as to minimize the seat transmissibility at the dominant frequencies of vertical vibration in the vehicle, taking account of the variation in sensitivity of people to vibration at different frequencies. This commonly involves the calculation of the SEAT value, either from the results of field tests or laboratory simulation with either subjects or dummies, or from mathematical simulation using the impedance of the seat and the impedance of the human body [3–8].

Apart from vertical vibration on the supporting surface of a seat, another main contributor to vibration discomfort in cars can be the fore-aft vibration on the backrest [2]. Few studies have investigated the transmission of fore-aft vibration through a seat backrest. Doolan and Mannino [9] measured seat back responses for four different seats using modal tests, resonance impact testing and multi-axis shaker table test methods. They observed different fore-aft resonance frequencies for the four seats, ranging from 6.3 to 19.75 Hz. The transmission of fore-aft vibration to a car seat has recently been studied in the field and in the laboratory [10,11]. In these studies, fore-aft and vertical vibration was measured at a single point at the seat base; a single-input single-output model and a two-input one-output model were employed to compute the vibration transmissibility of the seat. The results showed fundamental resonances of the seat backrest-person and the seat pan-person systems at about 4 or 5 Hz. The results also indicated that fore-aft vibration on the seat pan and the backrest were induced not only by fore-aft vibration at the car floor but also by vertical floor vibration, partly due to the inclination of the seat pan and backrest.

Due to rotational motions and non-rigidity of the car floor, the vibration may not be identical at the four corners by which a car seat is normally secured to the car floor. It was hypothesized that in order to better understand the transmission of vibration to the occupant of a car seat, the vibration should be measured at several positions at the seat base, and not only a single point. A multi-input model involving as many inputs as necessary should then be employed to compute the seat transmissibility.

This paper investigates the transmission of fore-and-aft, lateral and vertical vibration to the backrest of a car seat using multi-input methods. Vibration measurement was conducted in field tests in which the vibration inputs at the four corners of the seat and the vibration outputs at the backrest were measured in the three directions. Following the development of a suitable computer program, various multi-input models were employed to investigate the seat transmissibility in the fore-aft, lateral and vertical directions.

2. Vibration measurements and the motion at the seat base

2.1. Vibration measurements

Vibration measurements were undertaken in an experimental car (Ford Focus, Zetec, 2.0L, V817 LAR). The car was right-hand drive and had a mass of 1300 kg and a wheelbase of 2615 mm. The tests were made on a street road (in the City of Southampton, UK where driving is on the left) and in several other road conditions. Two subjects (drivers) participated in the tests. The weights and heights of the two subjects were 80 kg and 183 cm for subject A, and 70 kg and 170 cm for subject B. The driving speed was 35–45 miles per hour in the street road while the cars were in 4th gear. In this paper, only data associated with the street road condition obtained with subject A are presented (the data obtained with the other subject and in other driving conditions were broadly similar).

The installation of the transducers is shown in Fig. 1. A "SAE pad" conforming to ISO 10326-1 with built-in tri-axial accelerometers was used to measure accelerations on seat backrest in x, y and z directions. The pad, which weighed approximately 250 g including the built-in accelerometers, was fixed to the backrest using double-sided adhesive tape. Four transducer blocks were located in each corner of the seat base, as can be seen in Fig. 1, so as to measure accelerations at the four corners in the x, y and z directions. The four transducer blocks are identified as 1, 2, 3 and 4 in clockwise order starting from the front left corner. Each block was equipped with three piezoresistive accelerometers orientated in the three orthogonal directions. The four blocks were mounted such that they were co-axial with the four bolts that firmly pinned the seat rail to the car floor. The accelerometers were therefore mounted to the car floor; there was potential for free play due to gaps between the seat guide and the rail mechanism but this was small. Whereas the accelerometers used for blocks 1 and 2 (in the front of the seat base) were Entran EGCSY-240D*-10-type, miniature accelerometers Entran (EGA-125F*-10D/V10/L2M) were used for blocks 3 and 4 in order to accommodate the limited installation space encountered

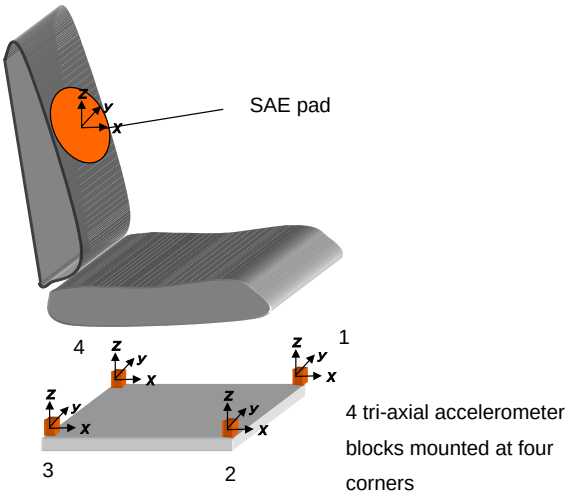

Fig. 1. Installation of SAE pads and accelerometers on the seat and the seat base.

at the rear of the seat base. In order to test whether the use of different types of transducers would influence the vibration measurements at the seat base, the 12 transducers were placed on the table of a vibration simulator and subjected to vertical random vibration (0.2–50 Hz). Transfer functions between each pair of transducers showed responses as expected. The measurements were also checked by comparison with data from a similar set of measurements (with a different transducer arrangement) in a parallel study.

So as to allow multi-input analysis, the input and output signals were measured simultaneously. In each test, a total of 15 acceleration signals (3 outputs from the seat backrest, plus 12 inputs from the seat base) were acquired to an *HVLab* data acquisition and analysis system (version 3.81). The test duration was 60 s and acceleration was sampled at 200 samples per second via 67 Hz anti-aliasing filters. Frequency analysis was performed for the acceleration inputs (at the seat base) and the acceleration outputs (at the backrest and the seat pan) after sampling the 60 s time histories at 200 samples per second to give 12,000 samples, which were divided into segments (with 100% overlapping) of 256 samples which were each multiplied by a Hamming spectral window. The frequency resolution was 0.78 Hz (i.e., 200/256) and there were 188 degrees of freedom (i.e., $4 \times 12000/256$).

Stationarity of the data was checked using a run test (a non-parametric approach) [12,13]. The 60 s records were divided into 20 time intervals of equal length. A mean square value for each interval was computed and the number of runs of mean square values above and below the median value of the series was counted. The results of this simple test suggested that the hypothesis of stationarity could be accepted for all signals ($p > 0.05$).

2.2. Vibration inputs at the seat base

Acceleration in the fore-aft direction at the seat base was mainly distributed over the frequency range from 5 to 30 Hz with a distinctive peak around 10 Hz (Fig. 2). Acceleration in the lateral

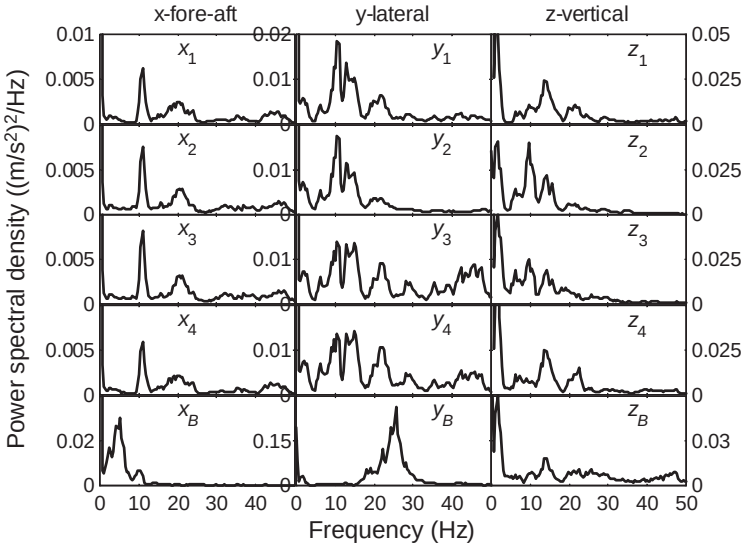

Fig. 2. Power spectral density functions measured in a street road, 35–45 miles per hour.

Table 1
Unweighted r.m.s. accelerations and frequency-unweighted VDV

Acceleration	r.m.s. (m/s^2)	VDV ($m/s^{1.75}$)
x_1	0.312	1.264
x_2	0.333	1.338
x_3	0.338	1.363
x_4	0.301	1.227
y_1	0.442	1.779
y_2	0.464	1.782
y_3	0.529	2.170
y_4	0.515	2.132
z_1	0.560	2.303
z_2	0.595	2.516
z_3	0.615	2.617
z_4	0.596	2.453
x_b	0.428	1.748
y_b	1.224	5.013
z_b	0.683	2.975

direction was rich in the frequency range 5–30 Hz. Moreover, there was vibration up to 50 Hz in the case of the rear lateral acceleration (y_3 and y_4). For vertical acceleration, the input vibration was rich in the frequency range 2–30 Hz.

For the power spectral density functions at the seat backrest (Fig. 2), the fore-aft acceleration is mainly in the range 1–10 Hz. In the lateral acceleration there is a peak around 25 Hz. The vertical acceleration is principally located in the frequency range below 40 Hz.

From Fig. 2, it can be seen that vibration inputs varied from corner to corner on the seat base. Table 1 lists the unweighted r.m.s acceleration and unweighted vibration dose values (VDV) computed from the measured signals. In general, the largest difference in the lateral acceleration is between the rear and the front of the seat base, while the differences between the fore-aft accelerations at the four corners seems to be less. For fore-aft acceleration, two signals (x_1 and x_4) at the left-hand side are similar and the other two (x_2 and x_3) at the right-hand side are similar (see Figs. 2 and 3). For lateral acceleration, a similar situation exists between the front signals (y_1 and y_2) and the rear signals (y_3 and y_4) with the latter appearing more obvious. For vertical vibration, the accelerations at the four corners were quite distinct from each other. The situation can be seen more clearly from inspection of the transmissibility between each pair of inputs.

Figs. 3–5 show the transmissibilities and corresponding ordinary coherence functions calculated between each pair of input signals in the fore-aft, lateral and vertical directions, respectively, using a single-input and single-output model. In these figures, H_{ij} represents the transmissibility from the acceleration at position i to the acceleration at position j. If the transmissibility between each pair of signals is different from unity, it means the vibration inputs at the seat base differed.

It can be seen from Fig. 3 that the two fore-aft accelerations at the left-hand side (x_1 and x_4) and the other two at the right-hand side (x_2 and x_3) are similar to each other (the transmissibility between the components in each pair is close to unity). Furthermore, coherencies between the signals x_1 and x_4 and between the signals x_2 and x_3 are close to unity, indicating high correlation

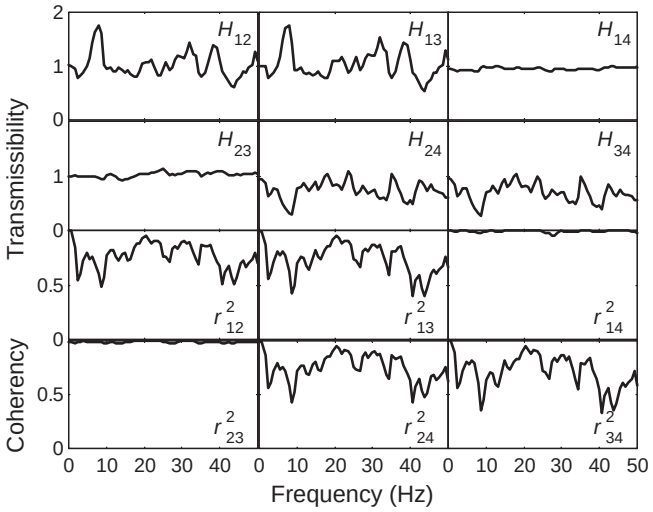

Fig. 3. Transmissibilities and coherencies between each pair of fore-aft seat inputs.

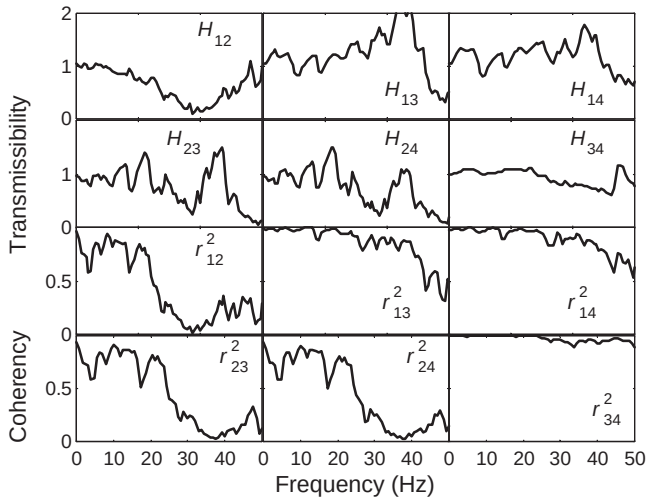

Fig. 4. Transmissibilities and coherencies between each pair of lateral seat inputs.

between the signals. In Fig. 4, a high correlation can be seen among the three lateral signals at the front left (y_1), the rear right (y_3) and the rear left (y_4) corners. Later, it will be seen that high correlation between inputs affects the calculation of seat transmissibility when using a multi-input model. Fig. 5 shows that the four vertical acceleration inputs were distinctly different from each other.

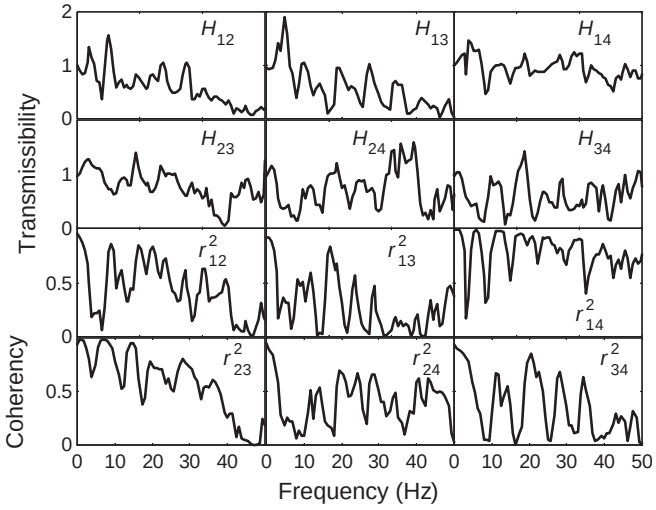

Fig. 5. Transmissibilities and coherencies between each pair of vertical seat inputs.

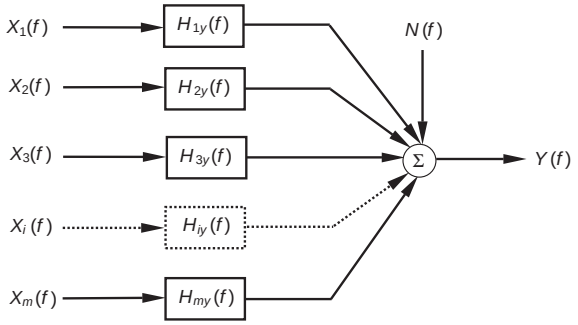

Fig. 6. Multi-input and single-output model for original inputs.

3. General multi-input and single-output model and computational algorithm

The general multi-input and single-output model for the original inputs is shown in Fig. 6, whereas an alternative conditioned multi-input and single-output model is shown in Fig. 7 [12]. In these figures, the terms $X_i(f)$, $i = 1, 2, \ldots, m$, are computed Fourier transforms from the original input signals $x_i(t)$. The terms $X_{i.(i-1)!}(f)$, $i = 1, 2, \ldots, m$, represent Fourier transforms corresponding to the conditioned inputs $x_{i.(i-1)}(t)$. For any i, the subscript notation $i.(i-1)!$ represents the ith record conditioned on the previous $(i-1)$ records, that is, when the linear effects of $x_1(t)$, $x_2(t)$, up to $x_{i-1}(t)$ have been removed from $x_i(t)$ by optimum linear least squares prediction techniques. Note that these ordered conditioned input signals are mutually uncorrelated. $H_{iy}(f)$ and $L_{iy}(f)$ (to be determined) are constant-parameter linear frequency response functions for the original and the conditioned inputs, respectively. The term $N(f)$ represents the Fourier transform of the unknown independent output noise and $Y(f)$ is the Fourier transform of the output signal $y(t)$.

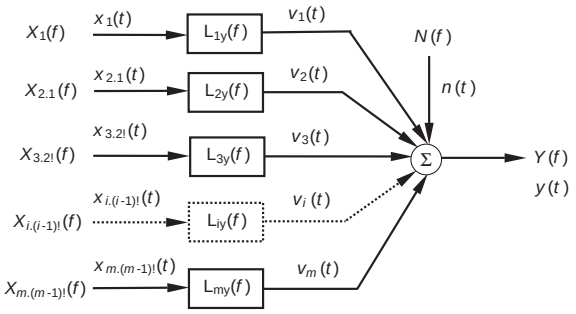

Fig. 7. Multi-input and single-output model for ordered conditioned inputs.

3.1. Conditioned spectral density functions and optimum systems for conditioned inputs

To compute the optimum systems (transfer functions) for the original and the conditioned inputs and the partial coherence functions, the conditioned spectral density functions are required:

$$G_{ij.r!} = G_{ij.(r-1)!} - L_{rj}G_{ir.(r-1)!}, \quad \text{for all } i > r \text{ and } j > r, \tag{1}$$

where $G_{ij.r!}$ are the conditioned cross-spectral density functions between $X_{i.r!}$ and $X_{j.r!}$, when $i \neq j$ with both $i > r$ and $j > r$. The constant-parameter linear system L_{rj} represents the optimum linear system to predict $x_j(t)$ from $x_r(t)$ taken in that order. From the above equation $\{G_{ij.r!}\}$ can be computed from knowledge of $\{G_{ij.(r-1)!}\}$ and the $\{L_{rj}\}$ systems. In particular, it shows that the $\{G_{ij.1}\}$ terms follow from knowledge of the $\{G_{ij}\}$ terms and the $\{L_{1j}\}$ systems. Then the $\{G_{ij.2!}\}$ terms follow from knowledge of the $\{G_{ij.1}\}$ and the $\{L_{2j}\}$ systems, and so on. The $\{L_{rj}\}$ systems are to be determined.

Since the inputs in Fig. 7 are mutually uncorrelated, each optimum system L_{iy} for conditioned input $x_{i.(i-1)!}(t)$ is defined by the ratio of the cross-spectral density function between its input and the output divided by the autospectral density function of its input:

$$L_{iy} = \frac{G_{iy.(i-1)!}}{G_{ii.(i-1)!}}, \quad i = 1, 2, \ldots, m. \tag{2}$$

The conditioned cross-spectral density functions $G_{iy.(i-1)!}$ between conditioned input $X_{i.(i-1)!}$ and output Y can be computed using following equation:

$$G_{iy.r!} = G_{iy.(r-1)!} - L_{ry}G_{ir.(r-1)!}, \quad \text{for all } i > r. \tag{3}$$

The conditioned autospectral density functions ($G_{ii.(i-1)!}$) of the conditioned input ($X_{i.(i-1)!}$) can be computed via the equation:

$$G_{ii.r!} = G_{ii.(r-1)!} - L_{ri}G_{ir.(r-1)!}, \quad \text{for all } i > r. \tag{4}$$

It is still necessary to determine the $\{L_{rj}\}$ systems. This can be done by extending the interpretation of the optimum $\{L_{iy}\}$ systems of Eq. (1) for the inputs X_1, $X_{2.1}$, $X_{3.2!}$ up to $X_{m.(m-1)!}$ with output Y. In place of Y, consider any output X_j, where $j = 1, 2, \ldots, (m+1)$. Let the inputs be X_1, $X_{2.1}$, $X_{3.2!}$ up to $X_{r.(r-1)!}$, where r can be any integer $r < j$, that is, $r = 1, 2, \ldots, (j-1)$.

Conceptually, this creates new conditioned multiple-input and single-output models where the associated optimum linear systems $\{L_{rj}\}$ through the derivation of the optimum $\{L_{iy}\}$ systems must be such that j replaces y and r replaces i to give the result:

$$L_{rj} = \frac{G_{rj.(r-1)!}}{G_{rr.(r-1)!}}, \quad r = 1, 2, \ldots, (j-1) \text{ and } j = 1, 2, \ldots, (m-1). \tag{5a}$$

3.2. Optimum systems for original inputs

The optimum linear systems $\{H_{iy}\}$ for the original inputs (Fig. 6) are in practice more complicated to compute than the optimum $\{L_{iy}\}$ systems. Fortunately, the difficulty can be overcome by deriving the relations existing between the $\{H_{iy}\}$ and $\{L_{iy}\}$ systems as below:

$$L_{iy} = \sum_{j=i}^{n} L_{ij} H_{jy}, \quad i = 1, 2, \ldots, m \text{ and } j \geqslant i. \tag{5b}$$

From this equation a general procedure to determine the $\{H_{iy}\}$ systems from the $\{L_{iy}\}$ systems by working backwards is thus established:

$$\begin{aligned} H_{my} &= L_{my}, \\ H_{iy} &= L_{iy} - \sum_{j=i+1}^{m} L_{ij} H_{jy}. \end{aligned} \tag{6}$$

3.3. Partial and multiple coherence functions

Having calculated the conditioned power spectral density functions in Eq. (1), partial and multiple coherence functions can be defined.

Ordinary coherence functions between any input x_i for $i = 1, 2, \ldots, m$ and the output y are defined by

$$\gamma_{iy}^2(f) = \frac{|G_{iy}(f)|^2}{G_{ii}(f) G_{yy}(f)}. \tag{7}$$

Partial coherence functions between any conditioned input $x_{i.1}$ for $i = 2, 3, \ldots, m$ and the output y are defined by

$$\gamma_{iy.1}^2(f) = \frac{|G_{iy.1}(f)|^2}{G_{ii.1}(f) G_{yy.1}(f)}. \tag{8}$$

Partial coherence functions between any conditioned input $x_{i.2!}$ for $i = 3, 4, \ldots, m$ and the output y are defined by

$$\gamma_{iy.2!}^2(f) = \frac{|G_{iy.2!}(f)|^2}{G_{ii.2!}(f) G_{yy.2!}(f)} \tag{9}$$

and so on up to

$$\gamma^2_{my.(m-1)!}(f) = \frac{|G_{my.(m-1)!}(f)|^2}{G_{mm.(m-1)!}(f)G_{yy.(m-1)!}(f)}. \tag{10}$$

Associated multiple coherence functions for any multi-input and single-output model can be determined in terms of the partial coherence functions. For the single-input and single-output model,

$$\gamma^2_{y:1}(f) = 1 - \left(\frac{G_{yy.1}(f)}{G_{yy}(f)}\right) = 1 - (1 - \gamma^2_{1y}) = \gamma^2_{1y}. \tag{11}$$

For the two-input and single-output model,

$$\gamma^2_{y:2!}(f) = 1 - \left(\frac{G_{yy.2!}(f)}{G_{yy}(f)}\right) = 1 - (1 - \gamma^2_{1y})(1 - \gamma^2_{2y.1}) \tag{12}$$

for the three-input and single-output model,

$$\gamma^2_{y:3!}(f) = 1 - \left(\frac{G_{yy.3!}(f)}{G_{yy}(f)}\right) = 1 - (1 - \gamma^2_{1y})(1 - \gamma^2_{2y.1})(1 - \gamma^2_{3y.2!}) \tag{13}$$

and so on. For an m-input and single-output model, the multiple coherence function is given by

$$\gamma^2_{y:m!}(f) = 1 - \left(\frac{G_{yy.m!}(f)}{G_{yy}(f)}\right) = 1 - \prod_{i=1}^{m}(1 - \gamma^2_{iy.(i-1)!}). \tag{14}$$

3.4. Computational algorithm

An algorithm for computing the vibration transmission to a car seat via a multi-input and single-output model based on Eqs. (1)–(4), (5a), (5b), (7), (10) and (14) was defined. The algorithm is described in Table 2.

Based on this algorithm, a computer program was developed using MATLAB (version 5.3). The program has a modular structure and consists of 12 modules with each individual representing a single-input and single-output model (after signal conditioning). Study of seat vibration transmission of an m-input and single-output model can be realized by calling first m modules via a master program. Up to 12 inputs can be available in the currently available program.

4. Seat vibration transmission via multiple input channels

The multi-input technique was employed to compute seat transmissibilities for the test car, using various models varying from single input to eight inputs. In the remainder of this paper, only the seat transmissibilities from the motion of the seat base to the motion of the backrest in the fore-aft, lateral and vertical directions are presented and discussed.

Table 2
Algorithm for a multi-input and single-output model

1	Define number of inputs m. Assign input signals to $x_1, x_2, \ldots, x_m$ and output signal to y.
2	Compute autospectral and cross-spectral density functions with the input and output signals to cover all the components: $\begin{bmatrix} G_{11} & G_{12} & G_{13} & \cdots & G_{1m} \\ & G_{22} & G_{23} & \cdots & G_{2m} \\ & & G_{33} & \cdots & G_{3m} \\ & & & \ddots & \vdots \\ & & & & G_{mm} \end{bmatrix}$, G_{yy} and $\begin{bmatrix} G_{1y} \\ G_{2y} \\ G_{3y} \\ \vdots \\ G_{my} \end{bmatrix}$.
3	Compute optimum system L_{1y} and ordinary coherency γ_{1y} for single-input and single-output model. Reserve the results and set $i = 2$ to proceed with next step.
4	For i-input and single-output model, compute conditioned spectral density functions $G_{ii.(i-1)!}$, $G_{iy.(i-1)!}$ and $G_{yy.(i-1)!}$ using Eqs. (1), (3) and (4), optimum systems L_{1i} up to $L_{(i-1)i}$ and L_{iy} with Eqs. (2), (5a) and 5(b) as well as partial coherency $\gamma^2_{iy.(i-1)!}$ with Eq. (10). Reserve the results for proceeding to next step.
5	Set $i = i + 1$ and go to step 4, until $i = m$.
6	Compute optimum systems H_{iy} $(i = 1, 2, \ldots, m)$ for the original inputs using Eq. (6) by working backwards and compute the multiple coherency $\gamma^2_{y:m!}$ using Eq. (14).

4.1. Transmissibility to the seat backrest in the fore-aft direction

4.1.1. From individual components of fore-aft vibration at the seat base to the fore-aft motion at the backrest: single-input and single-output model

Seat transmissibility from individual components of fore-aft vibration at the seat base to fore-aft vibration of the backrest was computed, first using a single-input and single-output model. Fig. 8 shows four sets of transmissibilities and coherencies calculated from the individual measures of fore-aft vibration at the four corners of the seat base. The results indicate that the transmissibility to the seat backrest differed between the four fore-aft vibration inputs at the seat base. The primary peak of the transmissibility occurs around 4–5 Hz. The coherence functions are poor: the coherencies are in most cases less than 0.5 over the frequency range (0–50 Hz) (Fig. 8).

It appears to be insufficient to consider only a single fore-aft input at the seat base when studying the transmission of fore-aft vibration to the seat backrest. The model should include the effect of all fore-aft input signals at the four corners of the seat base. Multi-input models are thus needed in order to take into account the effects of the multiple inputs on the vibration at the seat backrest.

4.1.2. From fore-aft inputs at the seat base to fore-aft output at the backrest: two-input and one-output model

The initial intention was to compute the fore-aft transmissibility of the seat backrest from fore-aft vibration at the four corners of the seat base. However, it has been noticed that the coherence functions between the input signals x_1 and x_4 on the left-hand side and between the signals x_2 and x_3 on the right-hand side were close to unity (Fig. 3), which means each pair of inputs contained

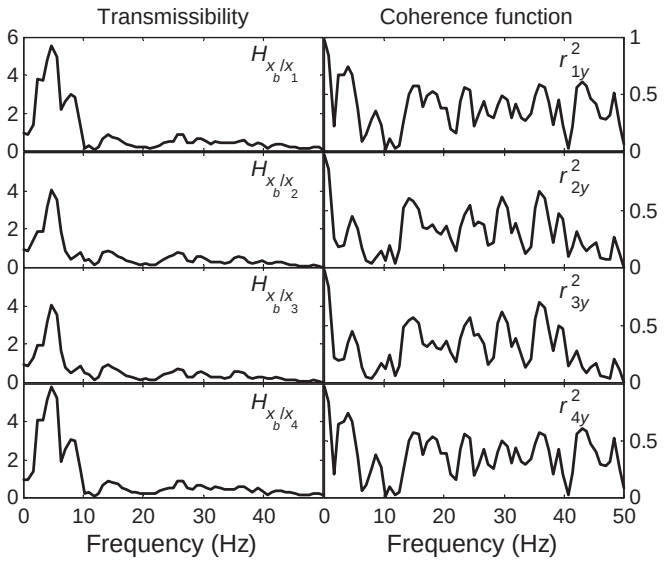

Fig. 8. Transmissibilities and coherencies from individual components of fore-aft vibration at the seat base to fore-aft vibration at the backrest using a single-input and single-output model.

redundant information. One of the pair of inputs should be excluded from the model in order to allow the distributed input systems to be studied as discrete inputs. Hence, a two-input and one-output model, making use of input signals x_1 and x_3, was adopted for this purpose.

With m input signals, it is possible to formulate a total of $m!$ different ordered conditioned multi-input and single-output models. For example, in the current 2-input and 1-output model, $m = 2$ will involve $2! = 2$ different models. When m is a large number the situation becomes extremely cumbersome and even intolerable. Fortunately, in practice, only a few possible orderings make physical sense. In the current case, the two inputs were arranged as x_1 and x_3. They are ordered according to the ordinary coherence functions between each input signal and the output signal in descending order over the frequency range of interest. In the remainder of this paper, input signal ordering will be given straightforwardly in a similar manner without re-mentioning unless indicated otherwise.

Computational results are shown in Figs. 9 and 10. A distinctive resonance can be seen at about 5 Hz from the resultant optimum systems for the original and the conditioned inputs (Fig. 9). The ordinary coherency (associated with input x_1) and the partial coherency (associated with input x_3) in Fig. 10 indicate that both inputs contributed to the fore-aft motion of the seat backrest. Comparing the multiple coherency (which shows how well the two inputs together linearly account for the measured output) in Fig. 10 with the coherence function obtained from single-input and single-output models (in Fig. 8), it can be seen that the vibration transmission of the backrest system was better represented by the two-input and one-output model than by the single-input and single-output models. However, because the above multiple coherency was not close to unity it implies that there must be some other causes of fore-aft backrest vibration that have not been taken into account.

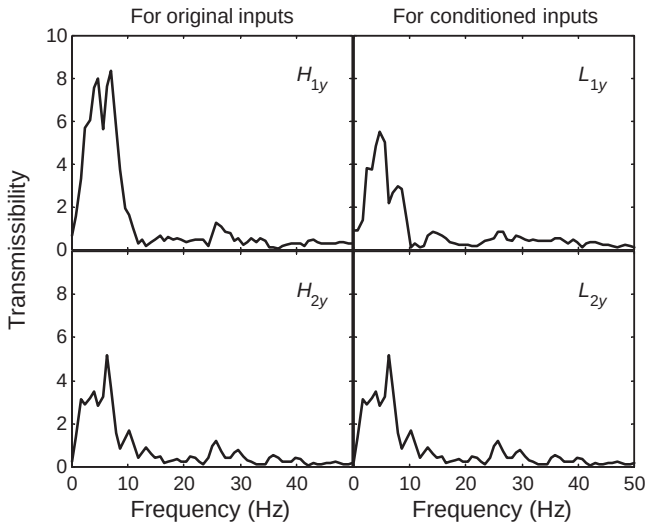

Fig. 9. Optimum systems for original and conditioned inputs, 2-input and 1-output model, for fore-aft output at the backrest.

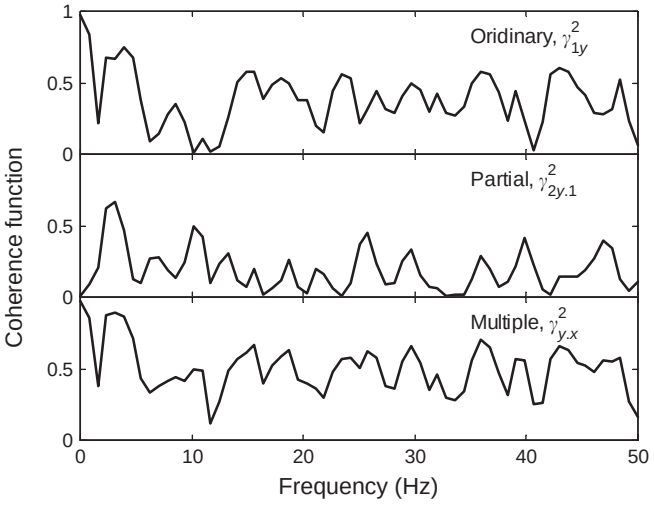

Fig. 10. Ordinary, partial and multiple coherence functions, 2-input and 1-output model, for fore-aft output at the backrest.

A previous study of vibration transmission to a car seat [9,10] showed that the poor coherency phenomenon encountered with a single-input and single-output model was also due to the inclination of the backrest. In other words, the transmissibility in one direction was not only induced by the input in that axis but also affected by vibration in another direction. To improve the coherence function, a more appropriate multi-input model that takes into account the above-mentioned cross-axis effect is considered.

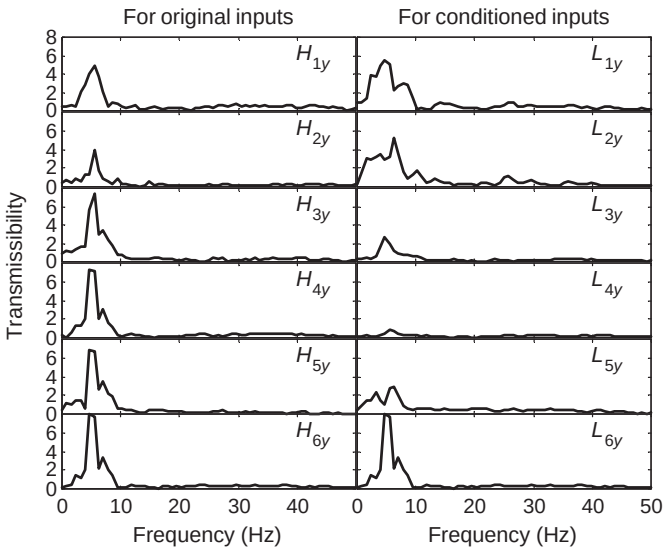

Fig. 11. Optimum systems for original and conditioned inputs, 6-input and 1-output model, for fore-aft output at the backrest.

4.1.3. From fore-aft and vertical vibration at the seat base to the fore-aft motion at the backrest: six-input and one-output model

A six-input and one-output model was adopted in which the six inputs were considered in turn as: the two fore-aft motions at the front left (x_1) and the rear right (x_3) corners and the four vertical motions at the rear left (z_4), the rear right (z_3), the front left (z_1) and the front right corners (z_2), respectively. The computed optimum systems for the original and conditioned inputs are shown in Fig. 11 and the ordinary, partial and multiple coherence functions are plotted in Fig. 12. While the characteristics (frequency content) of the transmissibilities remained similar to those from the single-input single-output and the two-input one-output models, the coherence function was significantly improved. It can be seen from the ordinary and partial coherencies in Fig. 12 that, in addition to the fore-aft input vibration, the four vertical motions of the seat base had a significant effect on the fore-aft motion of the seat backrest. Moreover, a very strong coherence (generally greater than 0.9) was observed in the multiple coherence function after adopting the six-input and one-output model.

4.1.4. From fore-aft, vertical and lateral vibration at the seat base to the fore-aft motion at the backrest: eight-input and one-output model

To check the effect of lateral inputs at the seat base on the fore-aft motion of the backrest, the above six-input and one-output model was extended to an eight-input and one-output model by including extra two lateral inputs (y_2 and y_3). The computational results are shown in Figs. 13 and 14. As can be seen from the corresponding partial coherence functions $\gamma^2_{7y.6!}$ and $\gamma^2_{8y.7!}$ in Fig. 14, that the lateral inputs had a rather small effect on the fore-aft motion at the backrest.

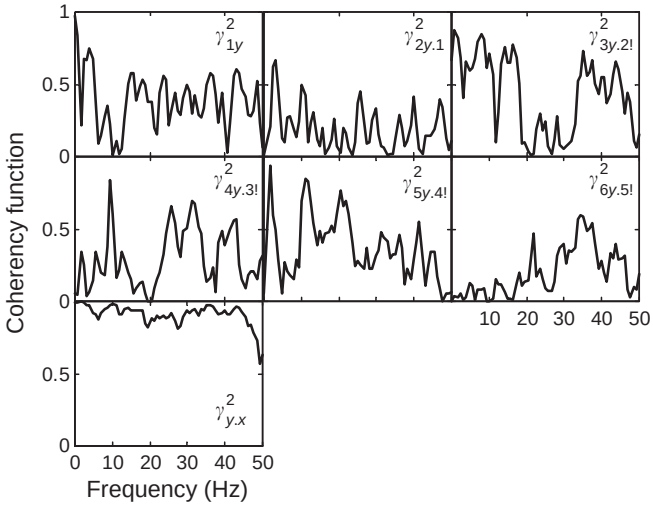

Fig. 12. Ordinary, partial and multiple coherence functions, 6-input and 1-output model, for fore-aft output at the backrest.

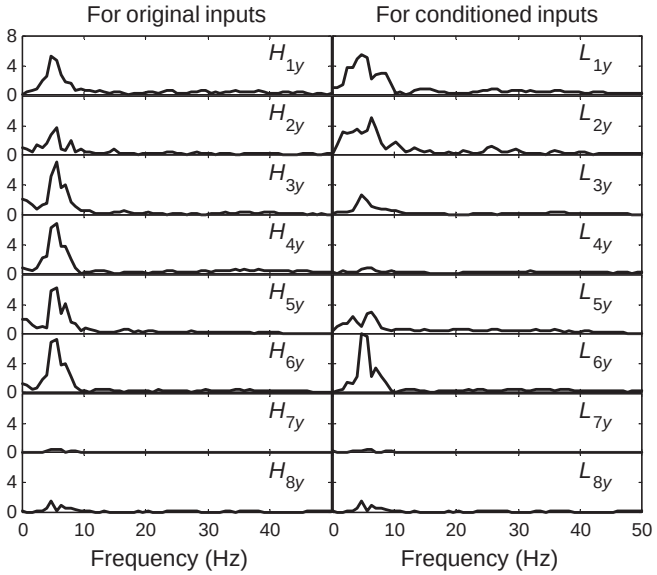

Fig. 13. Optimum systems for original and conditioned inputs, 8-input and 1- output model, for fore-aft output at the backrest.

4.2. Transmissibility to the seat backrest in the lateral direction

4.2.1. From individual components of lateral vibration at the seat base to lateral vibration at the backrest: single-input and single-output model

Seat transmissibility from the lateral vibration measured at each of the four corners at the seat base to the lateral vibration at the backrest was investigated using a single-input and single-output

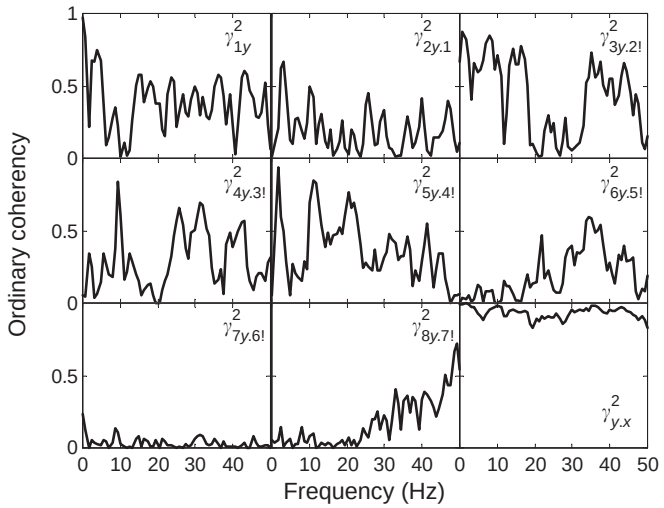

Fig. 14. Ordinary, partial and multiple coherence functions, 8-input and 1-output model, for fore-aft output at the backrest.

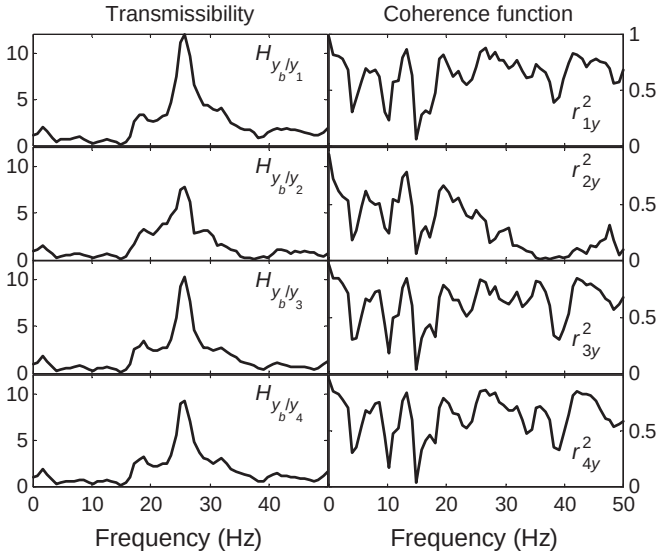

Fig. 15. Transmissibility and coherency from individual components of lateral vibration at the seat base to lateral vibration at the backrest using a single-input and single-output model.

model. The obtained transmissibilities and coherencies are shown in Fig. 15. As can be seen in this figure, for each lateral input the vibration at the backrest was amplified between about 18 and 35 Hz, with a distinctive peak around 26 Hz. The coherency was generally low.

4.2.2. From lateral inputs at the seat base to lateral output of the backrest: two-input and one-output model

A two-input and one-output model was adopted for studying the vibration transmission from lateral inputs (y_2 and y_3) at the seat base to the lateral output on the backrest. Lateral inputs y_1 and y_4 were not included since a high correlation was found among the three lateral signals at the front left (y_1), the rear right (y_3) and the rear left (y_4) corners (see Fig. 4). The computed optimum systems for the original and conditioned inputs and the ordinary, partial and multiple coherence functions are shown in Figs. 16 and 17. The characteristics of the transmissibility (Fig. 16)

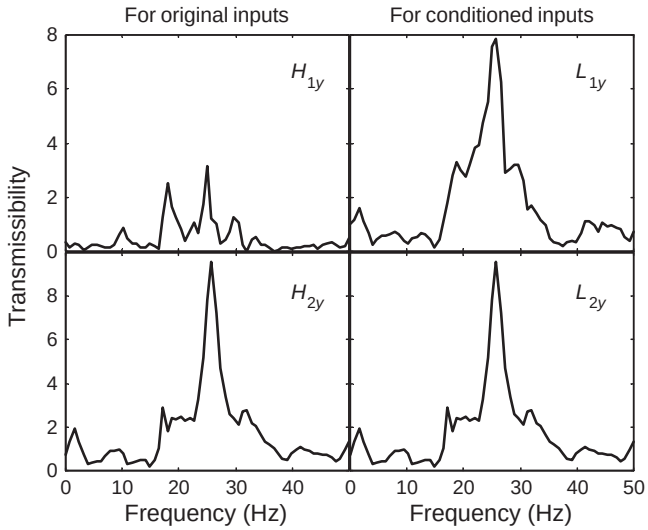

Fig. 16. Optimum systems for original and conditioned inputs, 2-input and 1-output model, lateral direction.

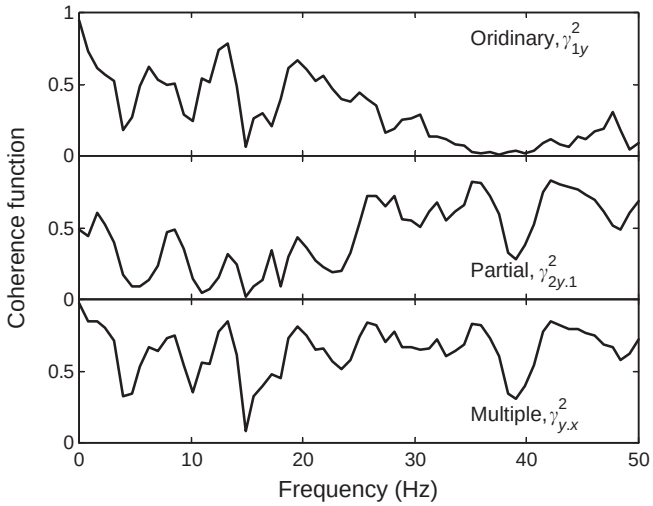

Fig. 17. Ordinary, partial and multiple coherence functions, 2-input and 1-output model, lateral direction.

appeared similar to that from the single-input model, with a distinctive resonance at about 26 Hz. From the multiple coherency in Fig. 17, it can be seen that the low coherency at low frequencies observed in the previous single-input model was slightly improved. One of the reasons for the coherency remaining low may be that some other input causing lateral vibration of the backrest, such as roll motion at the seat base, was not included. This will be investigated in future work [14].

4.3. Transmissibility to the seat backrest in the vertical direction

4.3.1. From individual components of vertical vibration at the seat base to vertical vibration at the backrest: single-input and single-output model

Seat transmissibility in the vertical direction was studied first using a single-input and single-output model. The transmissibilities and coherencies from individual components of vertical vibration at the four corners of the seat base to the vertical vibration at the backrest are shown in Fig. 18. Compared to the transmissibility in fore-aft and lateral directions from a single-input model, the ordinary coherency for vertical vibration was better, indicating that each vertical vibration at the four corners of the seat base was well correlated with the vertical vibration at the backrest. However, the four vertical transmissibilities to the backrest shown in Fig. 18 differ.

4.3.2. From vertical vibration at the seat base to vertical vibration at the backrest: four-input and one-output model

It is shown in Fig. 5 that all ordinary coherence functions between each pair of vertical inputs were well below unity at most frequencies. Since the four vertical inputs were not coherent with each other, they can have individual contributions to the vertical vibration at the backrest. A four-input (z_4, z_3, z_1 and z_2 in order) and one-output (z_b) model was thus adopted to study the

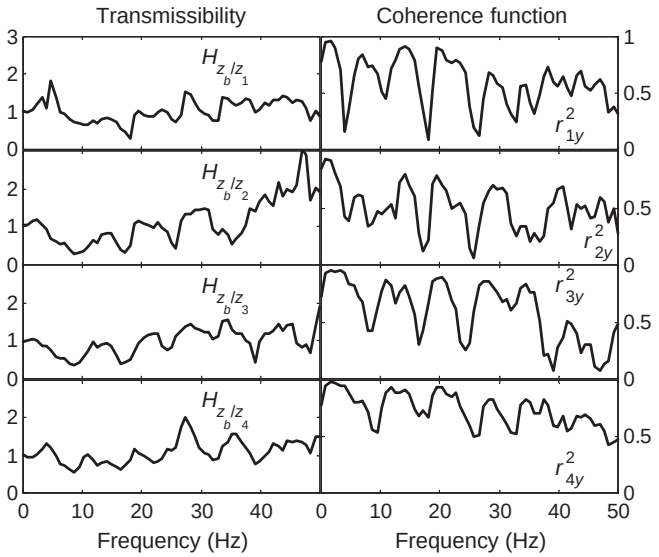

Fig. 18. Transmissibilities and coherencies from individual components of vertical vibration at the seat base to vertical vibration at the backrest using a single-input and single-output model.

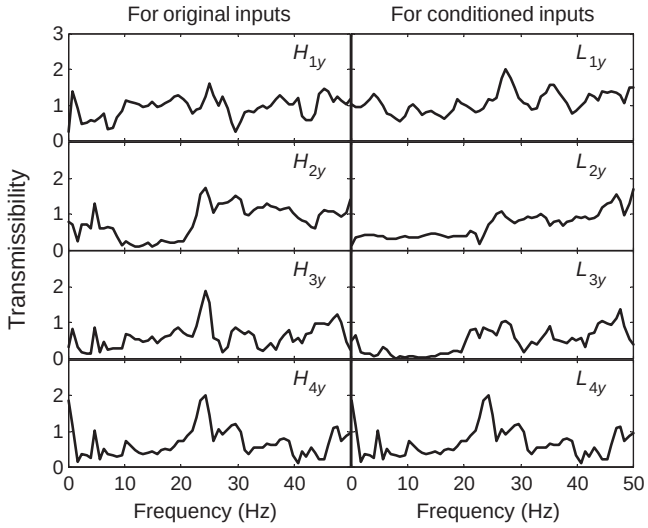

Fig. 19. Optimum systems for original and conditioned inputs, 4-input and 1-output model, vertical direction.

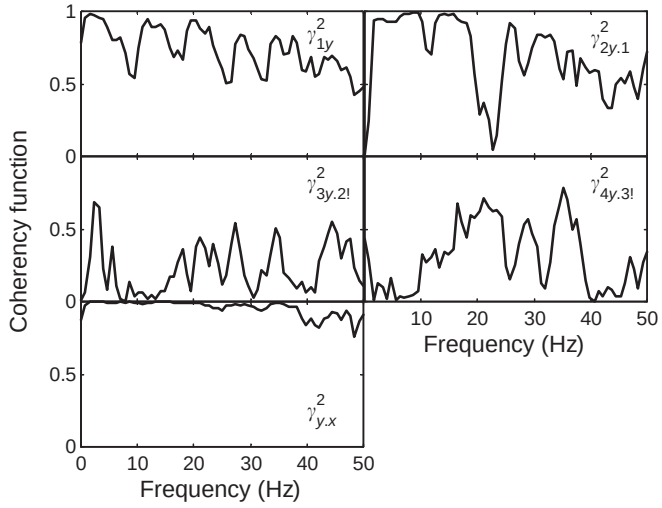

Fig. 20. Ordinary, partial and multiple coherence functions for 4-input and 1-output model, vertical direction.

vibration transmission to the backrest. Figs. 19 and 20 show the optimum systems for the original and conditioned inputs and various types of coherence functions computed using this model. It is noteworthy that a very high multiple coherence function was obtained (Fig. 20).

4.3.3. From vertical and fore-aft vibration at the seat base to vertical vibration at the backrest: six-input and one-output model

A six-input and one-output model for studying the transmission of vibration from the combined vertical and fore-aft inputs (z_4, z_3, z_1, z_2, x_1 and x_3) at the seat base to the vertical

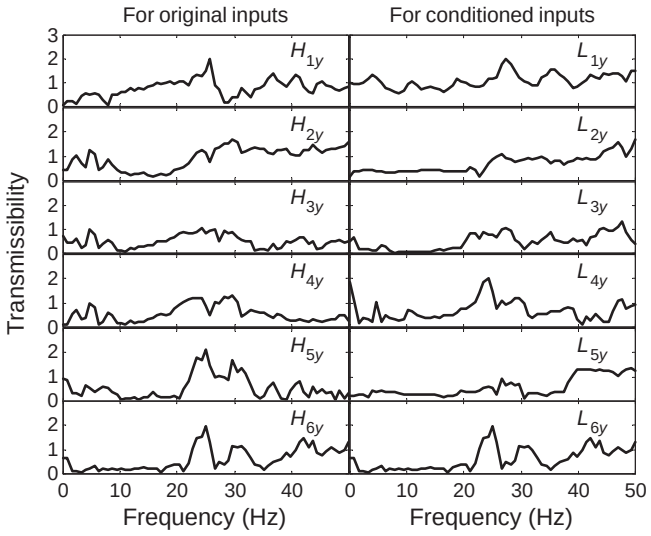

Fig. 21. Optimum systems for original and conditioned inputs, 6-input and 1-output model, for vertical output at the backrest.

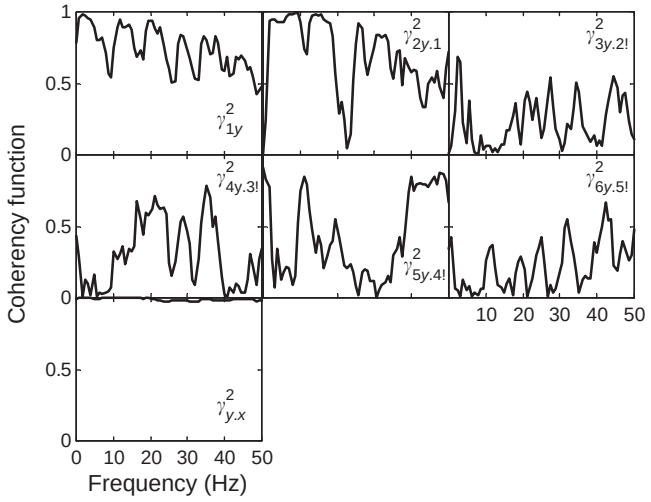

Fig. 22. Ordinary, partial and multiple coherence functions for 6-input and 1-output model, for vertical output at the backrest.

output at the backrest was adopted. The computed results from the model are shown in Figs. 21 and 22. The results show that vertical vibration at the backrest was caused not only by vertical vibration at the seat base but also by fore-aft vibration at the seat base. Each input considered in the current six-input model contributed to the output motion, as confirmed by the partial coherence functions in Fig. 22. An extremely good multiple coherency was obtained with this model.

4.4. Discussion

Refer to Fig. 7, for an illustrative diagram of an m-input and single-output model for conditioned inputs. Since the output terms $v_1(t)$, $v_2(t)$, …, $v_m(t)$ and $n(t)$ are mutually uncorrelated, the measured output auto-spectrum $G_y(f)$ is the sum of m auto-spectra terms, with no cross-spectra terms

$$G_y(f) = G_{v_1}(f) + G_{v_2}(f) + \cdots + G_{v_m}(f) + G_n(f), \tag{15}$$

where

$$\begin{aligned} G_{v_1}(f) &= |L_{1y}(f)|^2 G_{11}(f), \\ G_{v_2}(f) &= |L_{2y}(f)|^2 G_{22.1}(f), \\ G_{v_m}(f) &= |L_{my}(f)|^2 G_{mm.(m-1)!}(f). \end{aligned} \tag{16}$$

In the above equations, $G_{v_i}(f)\,(i = 1, 2, \ldots, m)$ is the auto-spectrum of the linear output $v_i(t)$ as shown in Fig. 7, $G_n(f)$ represents the auto-spectrum of the unknown noise $n(t)$, and $G_{ii.(i-1)!}(f)$ $(i = 1, 2, \ldots, m)$ indicates the auto-spectrum of the conditioned input $x_{ii.(i-1)!}(t)$ as computed in Eq. (4). It is possible to compute the auto-spectra $G_y(f)$ and the summation $\sum_{i=1}^{m} G_{v_i}(f) = G_{v_1} + G_{v_2} + \cdots + G_{v_m}$ and compare the two results. It is expected that the summation $\sum_{i=1}^{m} G_{v_i}(f)$ should be close to the output spectrum $G_y(f)$ if the m input signals have all contributed to the output signal.

The above calculation was carried out for: (i) the six-input one-output model of vibration transmission in the fore-aft direction (Section 4.1.3), (ii) the two-input one-output model in the lateral direction (Section 4.2.2), and (iii) the six-input one-output model in the vertical direction (Section 4.3.3). The auto-spectra $G_v(f)$ for the single-input and single-output model (which corresponds to $\sum_{i=1}^{m} G_{v_i}(f)$ in the m-input and one-output model) for the above three cases were also obtained. The results are presented in Figs. 23–25 for the three cases, respectively. For vibration transmission in the fore-aft direction, the single-input (x_1, fore-aft motion at the front

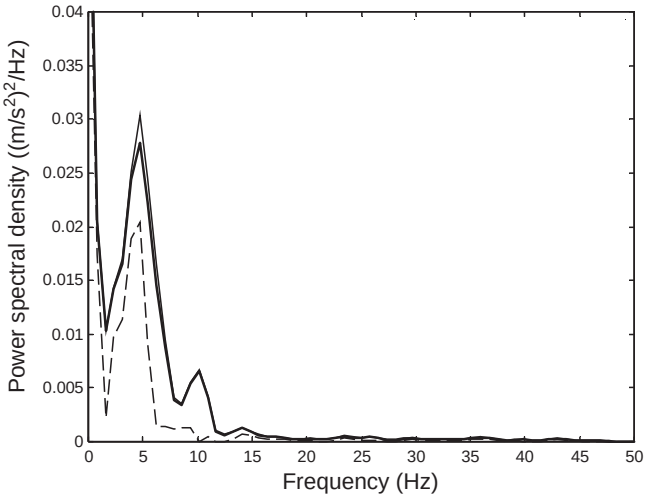

Fig. 23. Power spectral densities with single-input and six-input models for fore-aft vibration transmission in relation to Fig. 7. —— $G_{X_b}(f)$: output PSD; ---- G_v: one-input model; —— $\sum G_v$: six-input model.

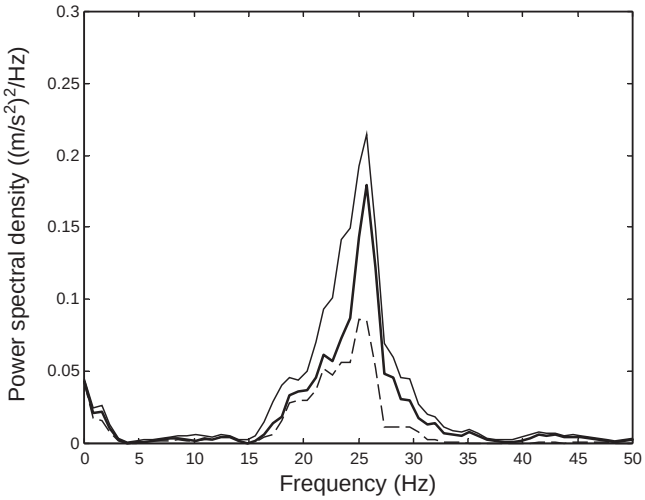

Fig. 24. Power spectral densities with single-input and two-input models for lateral vibration transmission in relation to Fig. 7. —— $G_{Y_b}(f)$: output PSD; ---- G_v: one-input model; —— $\sum G_v$: two-input model.

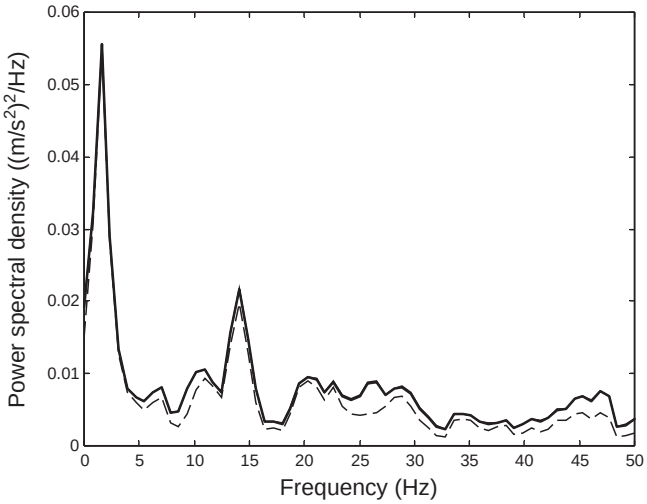

Fig. 25. Power spectral densities with single-input and six-input model for vertical vibration transmission in relation to Fig. 7. —— $G_{Z_b}(f)$: output PSD; ---- G_v: one-input model; —— $\sum G_v$: six-input model.

left corner of the seat base) model did not truly reflect the total of the vibration transmission from the seat base to the backrest. As can be seen in Fig. 23, there exists a large discrepancy between $G_v(f)$ (dashed line) and $G_{X_b}(f)$ (thin continuous line, the auto-spectrum of the fore-aft (output) motion at the backrest). However, the vibration transmission from the seat base to the backrest in the fore-aft direction was well represented by the six-input and one-output model, as may be seen from the close agreement between the two curves: $\sum_{i=1}^{6} G_{v_i}(f)$ (thick solid line) and $G_{X_b}(f)$ (thin continuous line).

In the lateral direction (see Fig. 24), the two-input model (y_2 and y_3, lateral motion at the front right and the rear right corners) better represented vibration transmission from the seat base to the backrest than the single-input model. However, the discrepancy between $\sum_{i=1}^{2} G_{v_i}(f)$ and $G_{Y_b}(f)$ is clear. It is again evident that lateral vibration at the seat base was not the only input source for lateral vibration at the backrest; transmission of rotational motion from the seat base needs to be considered.

In the vertical direction (in Fig. 25), the $\sum_{i=1}^{6} G_{v_i}(f)$ curve coincided almost exactly with the curve of the output auto-spectrum $G_{Z_b}(f)$. This means the six-input (z_4, z_3, z_1, z_2, x_1 and x_3) model almost perfectly represented the vibration transmission from the seat base to the backrest in the vertical direction. Even the single-input model yielded satisfactory results, as the difference between $G_v(f)$ and $G_{Z_b}(f)$ was rather small, especially at low frequencies.

The overall findings support the previous conclusion [10] that a single-input and single-output model is not sufficient to study vibration transmission to the backrest in the horizontal direction, while for vertical vibration transmission, the single-input model is sufficient, especially when low frequencies are of main concern.

5. Conclusions

The transmission of vibration in a car to the seat backrest via multi-input channels showed that vibration inputs in the fore-aft, lateral and vertical directions varied from position to position at the seat base. It was found that the two fore-aft accelerations at the left-hand side and the two fore-aft accelerations at the right-hand side of the seat base were highly correlated with each other. A similar situation existed for the two pairs of lateral accelerations on the left-hand side and the right-hand side of the seat base.

A computer program based on multi-input and single-output theory was developed to study the transmission of vibration to the seat backrest. The program, with a modular structure based on MATLAB, allows calculation of seat transmissibility with up to 12 different inputs.

Transmission of vibration to the seat backrest in the fore-aft direction was investigated using single-input single-output and multi-input single-output models. The results obtained when using a single-input model showed that the transmissibilities to the seat backrest from individual fore-aft vibration inputs at the four corners of the seat base were different. The primary peak of the transmissibility occurred around 4–5 Hz. The coherence function was low.

A two-input and one-output model that made use of the two least-correlated fore-aft input signals at the seat base was used to quantify seat transmissibility. Results showed that both inputs contributed to the fore-aft motion of the seat backrest. Nevertheless, the multiple coherency was not high, suggesting the need for a more appropriate multi-input model to include the cross-axis effect of vertical vibration, possibly caused by inclination of the backrest.

Allowing that the vibration on the seat in one direction may not only be induced by inputs in that axis, but may also be induced by vibration in other directions, a six-input and one-output model was employed with the six inputs being the two fore-aft motions and four vertical motions of the seat base. The coherence function was significantly improved.

An eight-input and one-output model was further introduced by adding the additional two least-correlated lateral inputs to the six-input model, in order to check the effect of lateral inputs

at the seat base on the fore-aft transmissibility of the backrest. As expected, results showed that the lateral inputs had a rather small effect on the fore-aft motion of the backrest.

Seat transmissibility from individual components of lateral vibration at the four corners of the seat base to the lateral vibration of the backrest was first investigated using a single-input and single-output model. Each lateral input vibration reaching the backrest in the same direction was amplified at frequencies from 18 to 35 Hz, with a peak around 26 Hz. The coherency was generally low but appeared higher at frequencies above 20 Hz. A two-input and one-output model was further adopted for studying the vibration transmission from lateral inputs at the seat base to the lateral output at the backrest. The characteristic of the transmissibility appeared similar to that with the single-input model. The low coherency at low frequency observed with the single-input model was improved. However, the improvement seemed limited by only considering translational vibration at the seat base. Rotational vibration may need to be considered in future work.

Transmissibility to the seat backrest in the vertical direction was first studied using a single-input and single-output model. The results showed that each of the four components of vertical vibration at the corners of the seat base was well correlated with the vertical vibration at the backrest. A four-input and one-output model was used to study the vibration transmission from vertical vibration at the four corners of the seat base. A very high multiple coherence function was obtained. A six-input and one-output model was further used to investigate vibration transmission from combined vertical and fore-aft inputs at the seat base to vertical vibration at the backrest. The results showed that the vertical motion on the backrest was affected not only by vertical but also by fore-aft vibration at the seat base.

The results are consistent with a previous finding that a single-input and single-output model is not sufficient to study vibration transmission to a backrest in the horizontal direction but, for the transmission of vertical vibration, a single-input model is applicable, especially when low frequencies are of most interest.

Acknowledgements

This research was funded by the Ford Motor Company Ltd. The authors would like to acknowledge the support of Jon Willey, Martin Jansz and Neil Dixon.

References

[1] M.J. Griffin, The evaluation of vehicle vibration and seats, *Applied Ergonomics* 9 (1) (1978) 15–21.
[2] C. Corbridge, M.J. Griffin, P. Harborough, Seat dynamics and passenger comfort, *Institute of Mechanical Engineers, Part F: Journal of Rail and Rapid Transit* 203 (1989) 57–64.
[3] M.J. Griffin, *Handbook of Human Vibration*, Academic Press, New York, 1996.
[4] T.E. Fairley, M.J. Griffin, Application of mechanical impedance methods to seat transmissibility, *Proceedings of International Conference on Noise Control Engineering, Internoise 83*, Vol. I, Institute of Acoustics, Edinburgh, 13–15 July 1983, pp. 533–536.
[5] T.E. Fairley, M.J. Griffin, The apparent mass of the seated human body: vertical vibration, *Journal of Biomechanics* 22 (1989) 81–94.

[6] T.E. Fairley, M.J. Griffin, The apparent mass of the seated human body in the fore-and-aft and lateral directions, *Journal of Sound and Vibration* 139 (2) (1990) 299–306.
[7] C.H. Lewis, M.J. Griffin, Evaluating vibration isolation of soft seat cushions using an active anthropodynamic dummy, *Journal of Sound and Vibration* 253 (1) (2002) 295–311.
[8] L. Wei, M.J. Griffin, The prediction of seat transmissibility from measures of seat impedance, *Journal of Sound and Vibration* 214 (1) (1998) 121–137.
[9] R.J. Doolan, V.F. Mannino, Comparison of seat system resonant frequency testing methods, SAE paper 951335, 1995.
[10] Y. Qiu, Measurement of fore-aft seat vibration transmissibility in a car, *Proceedings of the 36th UK Group Meeting on Human Response to Vibration*, DERA, Farnborough, UK, 12–19 September 2001.
[11] Y. Qiu, M.J. Griffin, Transmission of fore-aft vibration to a car seat using field tests and laboratory simulation, *Journal of Sound and Vibration* 264 (1) (2003) 135–155.
[12] J.S. Bendat, A.G. Piersol, *Random Data Analysis and Measurement Procedures*, 2nd Edition, Wiley-Interscience, New York, 1986.
[13] J.D. Gibbons, *Nonparameteric Methods for Quantitative Analysis*, American Sciences Press, Columbus, OH, 1985.
[14] Y. Qiu, M.J. Griffin, Transmission of roll, pitch and yaw vibration to the backrest of a seat supported on a non-rigid car floor, *Journal of Sound and Vibration*, in press.